https://doi.org/10.53964/jmbdd.2025005

https://www.innovationforever.com

Journal of
Modern Biology and Drug Discovery

ISSN 2788-8088 (Online)

Open Access

Research Article

Evaluation and Comparison of the Feasibility of Enzymatic Hydrolysis of Specific Mycotoxin Structures in the Active Sites of CPA and CbhA Enzymes using Molecular Docking Analysis and Molecular Visualization Graphic Tools

Rashid Akhundov[1*]

[1]Lomonosov Moscow State University, Department of Chemistry, Moscow, Russia

[*]**Correspondence to: Rashid Akhundov, Master of Chemistry,** Chemistry Department, Leninskie Gory, 1, building 3, Moscow Russia; Email: axundovrashid@gmail.com, axundovrashid@protonmail.com

Received: July 31, 2024 **Revised:** September 9, 2025 **Accepted:** September 19, 2025 **Published:** November 11, 2025

Abstract

Objective: This paper explores approaches to assess and compare the predicted enzymatic hydrolysis structures of specific mycotoxins in the active sites of CPA and CbhA enzymes using molecular docking analysis and molecular visualization and graphics tools.

Methods: The tools used in this work included: The ChemBio3D Ultra software package, extensible molecular visualization and modeling systems (EMVMS) PyMol and UCSF Chimera, and AutoDock Vina 1.1.2 molecular docking software.

Results: Visual binding of mycotoxins in the active centers of enzymes was shown, indicating possible enzymatic hydrolysis of ochratoxin A (OTA) in the active center of carboxypeptidase A (CPA) enzyme, as well as T-2 toxin and deoxynivalenol (DON) in the active center of cellobiohydrolase (CbhA) at the optimal pH (7.5 and 6, respectively) of enzyme action. Based on the results obtained from molecular docking using Autodock Vina 1.1.2 and EMVMSs UCSF Chimera and PyMol, it should be noted that according to the obtained affinities (kcal/mol), T-2 toxin binds best to the active site of CbhA enzyme (affinity value -7.8 kcal/mol); the next mycotoxin that binds best to the active site of CPA enzyme is OTA (affinity value -7.1 kcal/mol), followed by mycotoxin DON - to the active site of CbhA (affinity value -6.5 kcal/mol) at the optimal pH values of both enzymes.

Conclusion: The binding energies of specific enzyme substrates are slightly lower for most of the ligand poses compared to the values obtained for mycotoxins, providing their higher affinities**.**

Keywords: molecular docking, enzymatic hydrolysis, mycotoxin, enzyme, affinity, root mean square deviation (RMSD)

Citation: Akhundov R. Evaluation and Comparison of the Feasibility of Enzymatic Hydrolysis of Specific Mycotoxin Structures in the Active Sites of CPA and CbhA Enzymes using Molecular Docking Analysis and Molecular Visualization Graphic Tools. *J Mod Biol Drug Discov*, 2025; 4: 5. DOI: 10.53964/jmbdd.2025005.

https://doi.org/10.53964/jmbdd.2025005

1 INTRODUCTION

Mycotoxins as secondary metabolites are mainly produced by various types of fungi that affect agricultural raw materials and pose a global threat to public health. One of the most important mycotoxins in terms of toxicity and impact is OTA. OTA is a secondary metabolite produced by several species of *Aspergillus* and *Penicillium* fungi. The toxin, which is a nephrotoxic and nephrocarcinogenic compound, is mainly found in cereals but also in other foods such as coffee, wine, dried fruits, beer, and grape juice[1].

DON is also called vomitoxin because it can cause some of the typical acute effects, including nausea, vomiting, abdominal pain, diarrhea, headache, dizziness, or fever, which are also associated with outbreaks of gastroenteritis in animals and humans. In addition, DON acts as a potent inhibitor of protein synthesis and stimulates a pro-inflammatory response, which leads to the disruption of many physiological functions[2].

The T-2 toxin, trichothecene, is a sesquiterpene compound that is produced by the fungus *Fusarium* species and, under certain conditions, grows on crops in nature. The toxin is commonly found in crops such as corn, wheat, rice, and oats. T-2 toxin exhibits very stable chemical properties, mainly due to the presence of an epoxy group[3]. Therefore, if the epoxy group of DON and T-2 toxin is exposed, the toxicity of these mycotoxins will also be lost[4].

Recently, studies on the enzymatic degradation of mycotoxins with the help of various hydrolytic enzymes are relevant[5]. Therefore, for this study, those enzymes that have hydrolytic activity were selected. Enzymatic treatment is a convenient method for removing mycotoxins that involves the use of one or more enzymes. An important role in this is also played by the prediction of the possibility of mycotoxin degradation using various methods of molecular modeling[6]. This direction is still very important and interesting due to the fact that less toxic reaction products can be obtained as a result of enzymatic hydrolysis. Molecular modeling is a universal method that can be used in many areas of research, including the study of macromolecular structures[7]. As is known, molecular docking methods are aimed at predicting the most suitable way of binding a ligand to an enzyme[8].

Therefore, the purpose of this work is to determine the binding conformation of mycotoxins using molecular docking, as well as to conduct molecular docking for the description, visualization, and computer analysis of mycotoxins - OTA, DON and T-2 toxins as biostructures to predict their binding and enzymatic hydrolysis in the active centers of the enzymes CPA and CbhA.

To do this, it was necessary to carry out molecular docking of mycotoxins in the active center of some enzymes in order to identify their binding in the active center of enzymes, as well as to consider the mechanisms of enzymatic hydrolysis of mycotoxins. It should be noted that a review on the removal of various mycotoxins by enzymes was previously written[9].

UCSF Chimera is an interactive visualization and analysis tool for molecular structures and associated data, including density maps, trajectories, and sequence alignments[10,11], which can generate high-quality images. PyMol is a cross-platform open-source system based on Python[12]. This is a molecular graphics tool widely used for 3D visualization of proteins, nucleic acids, small molecules, electron densities, and surfaces.

It should be noted that there also exists UCSF Chimera X, the next-generation molecular visualizer from the Resource for Biocomputing, Visualization, and Informatics (RBVI) after UCSF Chimera[13-17], with the help of which it is possible to create 3D images of molecules, chemical structures, and different biomacromolecules. It should be noted that the advanced directions of protein design also lie in the construction of amino acid sequences and the incorporation of specific motifs, such as binding sites, into receptors, ion channels, or other proteins. This approach allows the production of protein variants with specific functions and purposes[18-20].

2 MATERIALS AND METHODS

Enzymes: carboxypeptidase A (CPA) (EC 3.4.17.1; PDB 1YME; Bos taurus) and cellobiohydrolase (CbhA) (EC 3.2.1.91; PDB 1RQ5; Clostridium thermocellum). Mycotoxins: ochratoxin A (OTA), deoxynivalenol (DON), T-2 toxin. Specific enzyme substrates: ((S)-hippurylphenyl-lactic acid or (S)-2-(2-benzamidoacetyl)-3-phenylpropanoic acid)); PNP-β-D-cellobioside (or 4-nitrophenyl cellobioside). Selected ligands for positive control: 4-chlorocinnamoyl-L-beta-phenyllactate and cellotetraose.

2.1 Work Methodology

Before proceeding with molecular docking[21], all structures of mycotoxins and specific enzyme substrates were optimized using Chem Bio 3D Ultra 12.0[22] and the minimization energy MM2[23,24]. Knowing the conformation of a ligand is important because the structure of a molecule often has a big impact on its reactivity. The goal of conformation optimization is to find an arrangement of atoms that makes the molecule as stable as possible. Molecules are most stable when their energy is low[23].

2.2 Procedure for Preparing Structures of Specific Substrates and Mycotoxins

All mycotoxin compounds and specific substrate structures were drawn in ChemBioDraw (version 12.0. CambridgeSoft). After that, energy minimization was

applied using ChemBio3D with the MM2 force field. The structures of the CPA and CbhA enzymes in PDB format were converted to PDBQT format using AutoDockTools (as part of MGLTools version 1.5.6., available at http://mgltools.scripps.edu/)[25-27] with atomic charges calculated by the built-in Gasteiger-Marsili. All enzyme structures in PQR format were converted to PDBQT format using AutoDockTools. Mycotoxins and specific substrate structures were attached to certain enzymes using the AutoDock Vina program (version 1.1.2. available at http://vina.scripps.edu/)[28,29]. The surface charge distribution of the CPA and CbhA enzymes at their optimal pH was calculated using the adaptive Poisson-Boltzmann solver (APBS. version 1.4.2.1) and the PDB2PQR servers (version 2.1.1) (available at http://www.poissonboltzmann.org/)[30,31] with force field PARSE and default settings. The mesh, the size of which was chosen in accordance with the size of the surface of the enzyme molecule, was approximately centered on the active sites of each of the enzymes. To perform the calculations, the program parameters were set by default, and 10 model poses of mycotoxin structures were selected. Affinities (kcal/mol) were obtained as the end result of molecular docking. The distances and angles between the atoms of the catalytic groups in the active site of the enzyme and the atoms of the mycotoxins were measured and visualized using extensible molecular visualization and modeling systems (EMVMS) PyMol (version 1.7.6. Schrödinger. LLC) and UCSF Chimera.

2.3 Molecular Docking Procedure

The procedure for performing molecular docking and obtaining enzyme-specific substrate and enzyme-mycotoxin complexes is as follows: before starting molecular docking. It is necessary to load the PDB files of the CPA and CbhA enzymes and the structures of all mycotoxins into the EMVMSs UCSF Chimera and PyMol. Remove excess heteroatoms from the enzyme structure. After which it is necessary to set the grid parameters. For example, for the PDB 1YME enzyme, these parameters were as follows: center_x=-3.324; center_y=26.215; center_z=-5.510; size_x=26; size_y=32; size_z=38. for PDB 1RQ5 enzyme: center_x=57; center_y=-8; center_z=-63; size_x=30; size_y=36; size_z=32. In each case, the exhaustiveness value was equal to 8, the number of binding modes - 10. The substrate binding position and conformation were determined by molecular docking using the Autodock Vina software.

2.4 Geometrical Optimization of Ligands

Before performing calculations, it may be necessary to optimize the geometry by identifying its stable conformations. Stable conformations can be found by performing energy minimization calculations. These calculations determine local and global minima of the energy of the model. Geometry optimization is iterative and starts from some initial geometry as follows:

The accuracy of the energy minimization calculations depends on the initial geometry, the potential energy function used, and the settings for the minimum allowed gradient between steps (convergence criterion). After an incremental change, ChemBio3D again determines the energy and energy derivatives and continues the process until convergence is reached, at which point the minimization process is terminated.

2.5 Energy Minimization with MM2

To minimize the energy of a molecule using MM2: (1) Set up optimal column dimensions in the Dimensions Table (go to View > Dimensions Table). (2) Go to Calculations > MM2 > Minimize Energy. (3) In the Energy Minimization dialog box, select any of the following options and click Run: Minimum Root Mean Square Gradient — Specify the convergence criteria for the gradient of the potential energy surface. Use larger values to reduce calculation time but obtain less accurate results. Use smaller values to improve the accuracy of your results but increase calculation time. (The default value of 0.100 is a reasonable compromise.) Display Each Iteration — Preview the model during calculation (displaying each iteration may slow down the calculation). Copy Dimensions to Output Window — Preview the value of each dimension in the Output Window. After calculating each new position, ChemBio3D moves each atom in a model so that the total energy is minimized. It is not possible to minimize energy in models containing phosphate groups depicted with double bonds.

For example, the paper[32] also notes that the two-dimensional structures of the synthesized compounds and the reference compound were constructed using ChemBioDraw Ultra 14.0 The three-dimensional structures of the ligands were protonated and optimized by the energy minimization method using the MM2 force field and 10,000 iterations of 2 femtoseconds. The conformationally optimized ligands were used for docking studies[32].

The scientific novelty of this study lies in the application and specific description of the mechanisms of action of enzymes using the approach of molecular docking of mycotoxins in the active centers of some enzymes, as well as in predicting the course of enzymatic hydrolysis and binding of mycotoxins in the active centers of enzymes, and this hypotheses is based on docking poses.

To determine the possibility of enzymatic hydrolysis, it is important and necessary to determine the targets in the structures of mycotoxin molecules. Breaking bonds in specific functional groups of mycotoxins is expected to lead to less toxic reaction products. Thus, in the structures of the known mycotoxins DON and T-2 toxin, such a target is the epoxy cycle, where, as a result of a nucleophilic attack in

https://doi.org/10.53964/jmbdd.2025005

Table 1. The Structure of the Molecules of Mycotoxins and Specific Substrates of Enzymes Selected as Objects of Study

Mycotoxins			Specific substrates	
OTA	DON	T-2 toxin	((S)-hippurylphenyl-lactic acid or (S)-2-(2-benzamidoacetyl) hydroxy-3-phenylpropanoic acid) (for CPA enzyme)	4-nitrophenyl cellobioside (for CbhA enzyme)
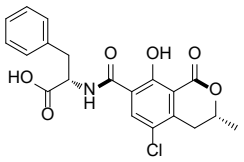	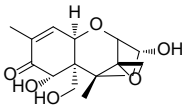	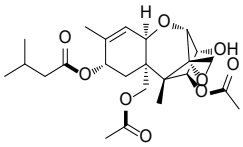	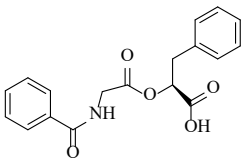	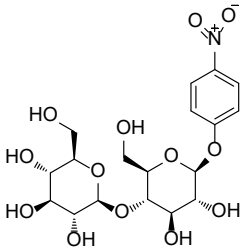

the active site of the CbhA enzyme, a simple C-O bond will break, and in the structure of the OTA mycotoxin, the amide group will occur (see Table 1). As a result of hydrolysis of the amide bond in the active site of the CPA enzyme, the C-N bond breaks.

3 RESULTS

As an illustration of mycotoxin binding, Figure 1A shows the resulting OTA conformation at the CPA active site. It should be kept in mind that docking gives only an approximate position of the substrate in the active site of the enzyme. As a result of calculations performed in EMVMSs UCSF Chimera and PyMol at a distance of 4 Å from the surface of mycotoxin molecules, amino acid residues included in the active center of the enzyme, with which functional groups can potentially interact, were isolated. In the case of the CPA enzyme, as well as for the CbhA enzyme, the attacking nucleophile is a water molecule.

The results of angles of attack and distances for OTA are shown below in Tables 2 and 3.

Table 4 summarizes the obtained nucleophilic attack angles and distances measured from the O atom of the water molecule to the C atom in the structures of the mycotoxins DON and toxin T-2, as well as from the O atom of the amino acid residues Asp383, Asp386 to the H atom of the water molecule in the active center of the enzyme CbhA in both EMVMSs.

CPA is a proteolytic enzyme that hydrolyzes a peptide bond at the carboxy-terminal (C-terminus) end of a protein or peptide. The zinc atom forms coordination bonds in the form of a tetrahedron with the side chains of two amino acid residues, His69 and His196 of the main chain of the CPA enzyme, the side chain of glutamic acid, Glu72, and a water molecule. The fourth coordination bond is occupied by a water molecule.

The Zn^{2+} ion coordinated with the residues of the CPA active center activates the water molecule, which, in full accordance with the known mechanism of enzyme action[33], carries out a nucleophilic attack on the carbon atom of the amide bond of the substrate. Some coordination of the Zn^{2+} ion is possible with the oxygen atom of the same amide group. As a result of the rearrangement of bonds in this amide group, the C-N bond is broken (see Figures 1B and 2B) with the formation of a phenylalanine leaving group. The subsequent interaction of the formed complex with a water molecule activated by the Glu270 residue leads to the release of ochratoxin-α and the restoration of the initial state of the enzyme. The interaction of zinc with the oxygen of the carbonyl group strongly polarizes the C=O bond, and the nonpolar environment of zinc enhances its ability to induce a dipole. The proximity of the negatively charged carboxyl group of Glu270 also contributes to the strong polarization of the carbonyl group.

The mechanism shown above involving a water molecule was proposed on the basis of X-ray diffraction studies of the CPA enzyme complexes formed with slowly hydrolyzed substrates and transition state analogue inhibitors. The promoted water mechanism assigns a dual role to the Glu270 residue. In the initial step of nucleophilic addition, Glu270 serves as a common scaffold to facilitate the nucleophilic attack of zinc-bound water on the mobile carbonyl carbon by transferring a proton from the water molecule to the oxygen atom of the carboxyl group. In the second cleavage step, Glu270 acts like an ordinary acid, donating this proton to the leaving nitrogen group. Thus, Glu270 carboxylate functions as a base, separating a proton from a water molecule bound to a zinc ion to generate a nucleophilic hydroxide ion, which in turn attacks the carbonyl carbon of the peptide bond, creating a tetrahedral transition state. The nucleophilic pathway, which is not viable in proteolytic reactions, results in a stable acyl-enzyme complex[34,35].

https://doi.org/10.53964/jmbdd.2025005

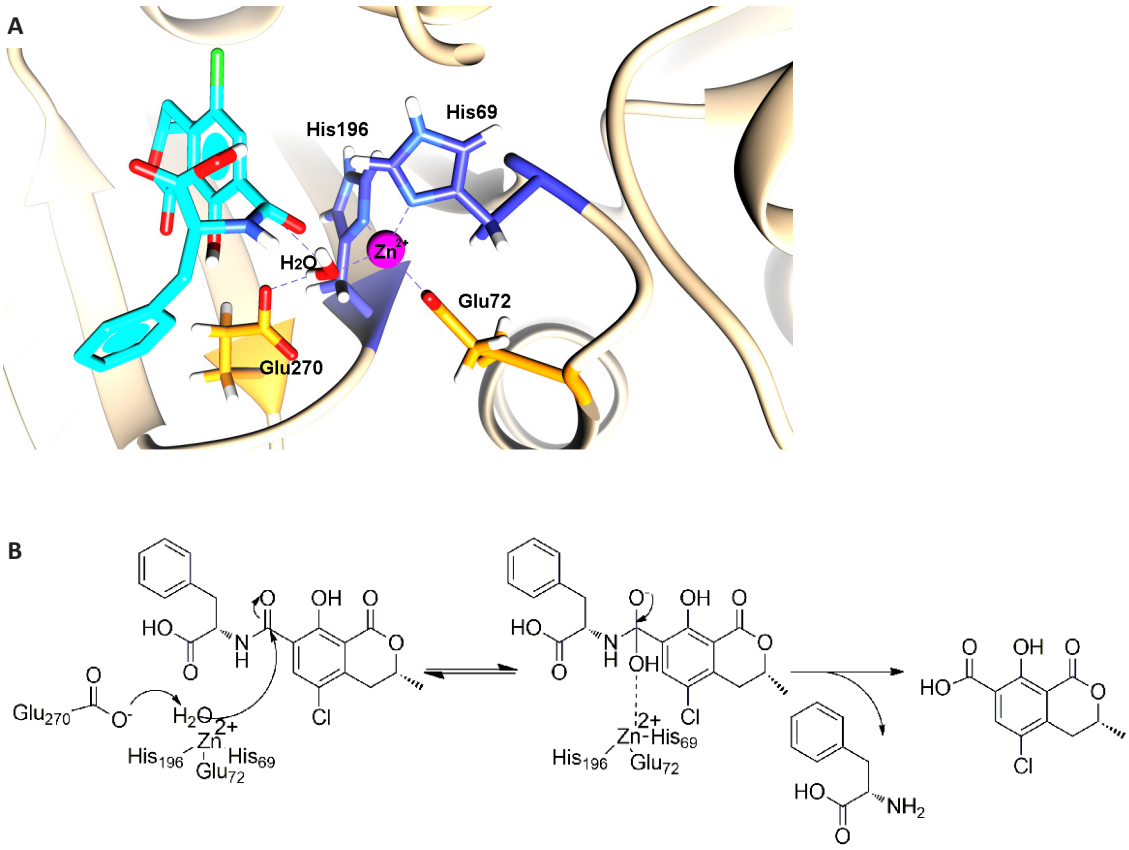

Figure 1. Binding of OTA in the Active Site of the CPA Enzyme at the Optimum pH 7.5 of the Enzyme (A) and the Proposed Mechanism of Enzyme Action (B). The Picture was Obtained as a Result of Molecular Docking using EMVMS UCSF Chimera: Zn^{2+} ion, Catalytically Important Residues: His196 and His69, Glu72 and Glu270. The Dotted Lines Show the Supposed Interactions of the Catalytically Important CPA Residues and the Zn^{2+} ion with the Amide Bond in the OTA Structure.

Table 2. Values of the Angle of Nucleophilic Attack and Distances Measured from the O Atom of the Water Molecule to the C Atom in the OTA Structure and the Zn^{2+} Ion, as well as from the O Atom of the Glu270 Amino Acid Residue to the H Atom of the Water Molecule in the Active Site of the CPA Enzyme in EMVMS UCSF Chimera

Distances, Å
H_2O---C=3.5
O_{Glu270}---H_{HOH}= 1.8
H_2O---Zn=1.9
Angle
H_2O--C--N=126°

Table 3. Nucleophilic attack angle and distances measured from the O atom of the water molecule to the C atom in the OTA structure and the Zn^{2+} ion, as well as from the O atom of the Glu270 amino acid residue to the H atom of the water molecule in the active site of the CPA enzyme in EMVMS PyMol

Distances, Å
H_2O–C=1.3
O_{Glu270}–H_{HOH}=3.3
H_2O–Zn=3.7
Angle
H_2O–C–N=97.2°

Based on the obtained Figures 1B and 2B, we can say that the mechanism of action of the CPA enzyme is close to the real mechanism, because in both cases the C-N bond is broken and the reaction product ochratoxin-α is formed.

In accordance with the known mechanism of enzyme action[36], the catalytic mechanism of CPA in the case of a specific substrate (S) - hippurylphenyllactic acid - is initiated by the nucleophilic attack of the Glu270 carboxylate on the carbonyl carbon of the bound substrate with the formation of an anhydride intermediate. The intermediate anhydride is then hydrolyzed by the zinc bound water molecule at the active site to give CPA-regenerated products. This reaction route is commonly referred to as the anhydride mechanism (Figure 3).

The active site of the CbhA enzyme has 3 catalytically important amino acid residues: Asp383, Asp386, and Gln795. While Gln795 is believed to stabilize the transition state, Asp383 is believed to deprotonate the water molecule[37,38], which carries out a nucleophilic attack on the nearest carbon atom of the epoxide ring of the mycotoxin DON and T-2 toxin molecules (see Figures S1-S4).

The enzyme CbhA has its pH optimum range at 6.0, at

https://doi.org/10.53964/jmbdd.2025005

Table 4. Nucleophilic attack angles and distances measured from the O atom of the water molecule to the C atom in the structures of mycotoxins DON and T-2 toxin, as well as from the O atom of the amino acid residues Asp383, Asp386 to the H atom of the water molecule in the active site of the CbhA enzyme in both EMVMSs

PyMol		UCSF Chimera		PyMol		UCSF Chimera	
Distances, Å	Angle	Distances, Å	Angle	Distances, Å	Angle	Distances, Å	Angle
Mycotoxin DON				Mycotoxin T-2 toxin			
H_2O—C= 3.0	H_2O–C–O= 139.7	H_2O—C=3.49	H_2O–C–O=111 °	H_2O—C=3.4	H_2O–C–O= 108,6°	H_2O—C=3.6	H_2O–C–O= 55°
O_{Asp383}—H_{H2O}= 3.0		O_{Asp383}— H_{H2O}= 2.3		O_{Asp383}— H_{H2O}= 3.0		O_{Asp383}—H_{H2O}= 2.3	
O_{Asp386}—H_{H2O}= 2.7		O_{Asp386}— H_{H2O}= 1.9		O_{Asp386}— H_{H2O}= 2.7		O_{Asp386}—H_{H2O}= 1.9	

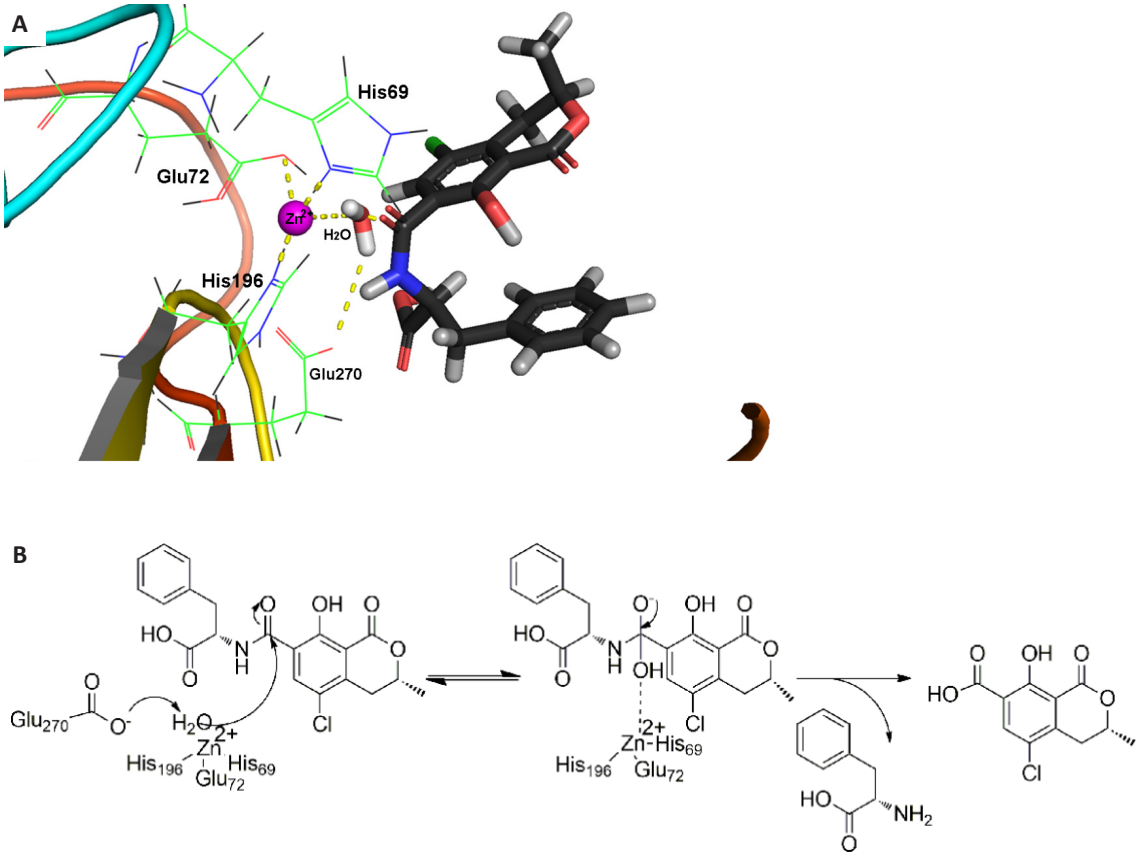

Figure 2. OTA binding in the active site of the CPA enzyme at the optimum pH 7.5 of the enzyme (A) and the proposed mechanism of enzyme action (B). (ochratoxin-a picture obtained using PyMol EMVMS: Zn^{2+} ion, catalytically important residues His196, His69, Glu72, and Glu270) The dotted lines show the putative interactions of the catalytically important CPA residues and the Zn^{2+} ion with the peptide bond in the OTA structure.

which one of these aspartates is protonated whereas the other aspartate is deprotonated. If the pH value is lowered to more acidic conditions, both aspartates Asp383 and Asp386 become protonated. Thus, different pH values can alter the protonation states of ionizable residues, which can lead to a conformational change on either the protein or the protein-ligand complex. Most of the protonation effect based on our calculations occurs at the catalytic dyad. Since Asp383 and Asp386 behave like a dicarboxylic acid due to the given structural conditions and the small distance between them, Asp386 is most likely protonated at pH 7.0, whereas no change for the catalytic triad occurs at pH 6 during complex formation. Novel crystal structures at higher pH values reveal no major conformational changes; soaking at pH 7.5 results in a modified orientation compared to the structure in the acidic range. Although there is a tiny residual density for the ”acidic” conformation at pH 7.5 and vice versa, these are negligible.

The enzymatic activity experiences a pK around 6 which is ascribed to the ionization of Glu270. Anions are capable of replacing the coordinated water in the latter cases and for the case where Glu 270 is protonated.

The present calculations are significant, for any proposed enzymatic mechanism, in the absence of a low-pH structure of CPA enzyme due to instability of the protein crystals at pH value lower than 7. By comparing the evolution of the

https://doi.org/10.53964/jmbdd.2025005

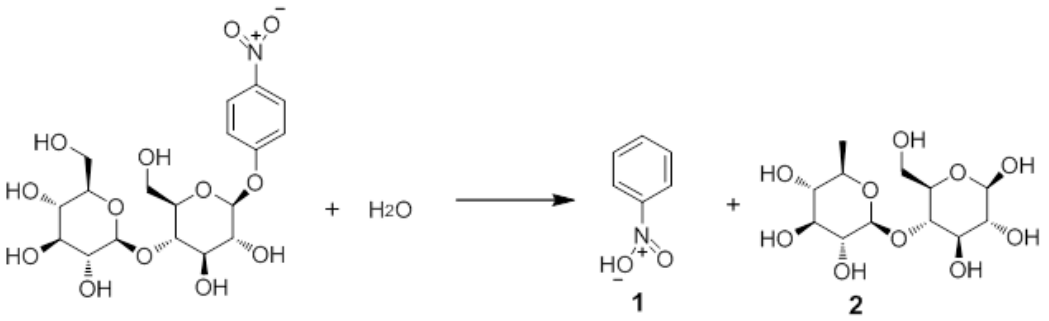

Figure 3. Hydrolysis of the Specific Substrate 4-nitrophenyl Cellobioside by the CbhA Enzyme to form 4-nitrophenol (1) and Cellobiose (2).

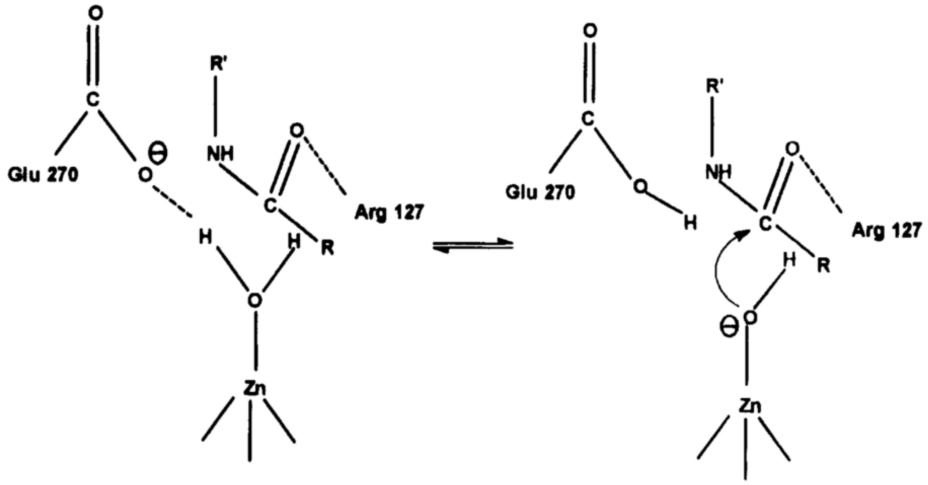

Figure 4. The Scheme of the Protonation of Catalytic Residue Glu270[39].

distances in the cases of deprotonated and protonated enzyme (CPA and CPAHl), we can see an increase in distance between Glu270 and the zinc-bound water molecule upon protonation of the former group.

Also in CPAH2 a movement of Glu270 away from the zinc-bound water is observed. The inactivity of the acidic form of the enzyme is easily consistent since a protonated Glu is disfavored in the formation of an anhydride. The protonation of Glu270 breaks a catalytically important hydrogen bond with the zinc-bound water and accounts for the enzyme becoming inactive at low pH. However, it is also completely consistent with the mechanism: the protonation of Glu270 breaks a catalytically important hydrogen bond with the zinc-bound water and accounts for the enzyme becoming inactive at low pH. The present picture is a sound model for further investigations of the action of CPA enzyme. Figure 4 shows the protonation scheme of the catalytic residue Glu270.

The investigation[39] has therefore proposed a reliable picture of the enzyme in the inactive acidic form. The movement of Glu 270 in the protonated CPAH enzyme is similar to that found when an amino acid binds the enzyme with the carboxylate group interacting with Arg 145. The Glu270-water interaction is broken, and a new interaction occurs between Glu 270 and the amino group of D-Phe. Upon breaking of the carboxylate-water bond, the zinc-bound water becomes easily displaced by anions.

Protonation of Glu270 also induces a minor solvation of the active site, the water molecules present in the cavity being fewer in the CPAH enzyme than in CPA. GluH270 still hydrogen-bonds with some water molecules during the dynamics, but these water molecules are highly mobile and move rapidly in and out during the trajectory. GluH270, in the new position far from the zinc ion, is not interacting significantly with other residues of the protein; its movement should be ascribed essentially to electrostatic factors. The extra positive charge present on the GluH270 residue strongly reduces the energy of interaction between the negative deprotonated Glu270 and the positive active-site zinc ion in the native CPA enzyme.

It is known that many programs, including AutoDock Vina, keep cyclic structures rigid during molecular docking. The AutoDock Vina 1.1.2 program is faster compared to some programs[26] and provides better and more accurate explanations for the obtained results of enzyme docking and the applied ligands than those provided by the AutoDock 3.0 program[40]. Based on the data of[41,42], it can be noted that the AutoDock Vina and AutoDock 4 programs find ligand posture models as a result of molecular docking within 2.0

https://doi.org/10.53964/jmbdd.2025005

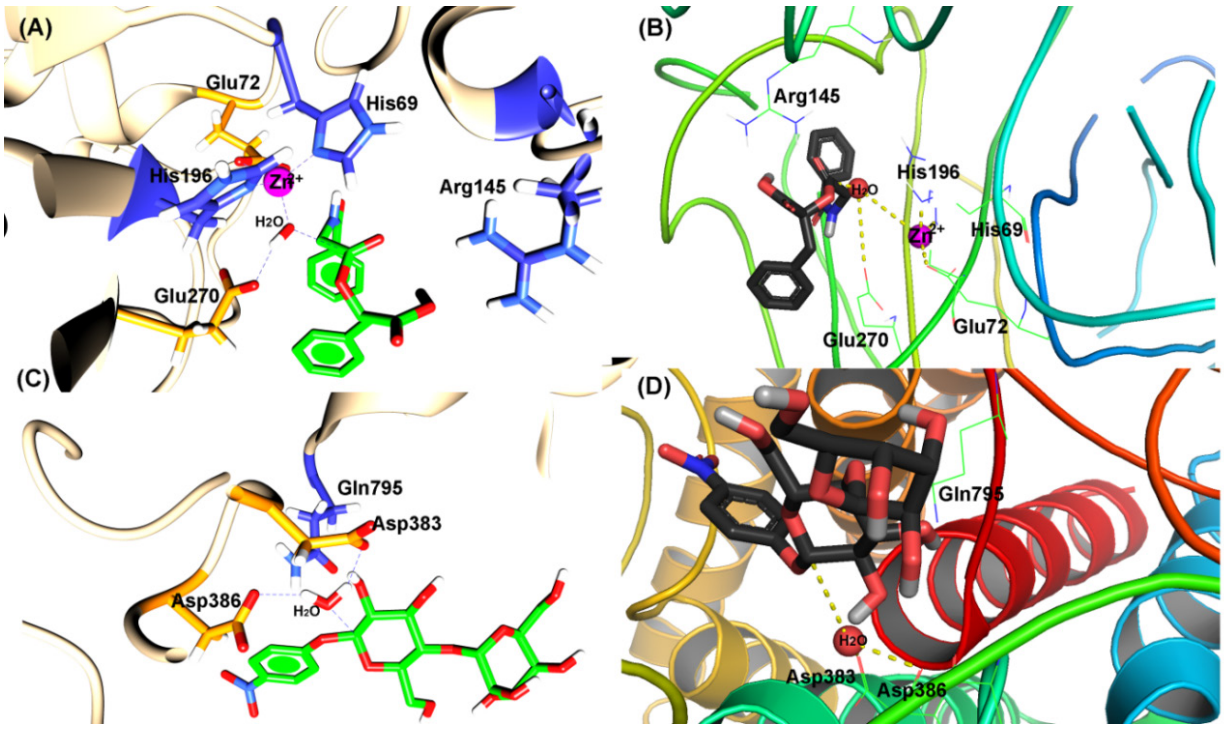

Figure 5. Binding of a specific substrate (S) - hippurylphenyl lactic acid in the active site of the CPA enzyme at the optimum pH 7.5 of the enzyme, obtained using UCSF Chimera (A) and PyMol (B) EMVMS and 4-nitrophenyl cellobioside in the active site of the CbhA enzyme at the optimal pH 6 action of the enzyme, obtained using UCSF Chimera (C) and PyMol (D). The dotted lines show the putative interactions of the catalytically important residues of the CPA and CbhA enzymes with functional groups in the structures of specific substrates.

Å RMSD for approximately 35% of the test set. AutoDock Vina finds ligand positions within 4.5 Å RMSD for almost 90% of the structures in the test set, but the percentage of these results in AutoDock 4 is much lower at about 55%. The resulting Figure 5 shows the binding of the specific substrate (S) - hippurylphenyllactic acid in the active site of the CPA enzyme at the enzyme's optimal pH of 7.5, obtained using EMVMSs UCSF Chimera (A) and PyMol (B) and 4-nitrophenyl cellobioside in the active site of the CbhA enzyme at the enzyme's optimal pH 6.

Usually, in order to predict the presence or absence of catalysis, it is important to refer to data obtained with specific enzyme substrates. The results of angles of attack and distances for these substrates are shown in Table 5.

In order to validate the molecular docking protocol and RMSD calculations, a positive control was performed, namely, molecular docking of two additionally selected as an example ligands - cellotetraose (in the case of the CbhA enzyme) and 4-chlorocinnamoyl-L-beta-phenyllactate[43] (in the case of the CPA enzyme) (see Table 6). Figure 6 shows the binding of the 4-chlorocinnamoyl-L-beta-phenyllactate in the active site of the CPA enzyme at the enzyme's optimal pH of 7.5, obtained using EMVMSs UCSF Chimera (A) and PyMol (B) and cellotetraose in the active site of the CbhA enzyme at the enzyme's optimal pH 6 also using both EMVMSs.

4 DISCUSSION

For the specific substrates of both enzymes mentioned above, the presence of catalysis in the active site has already been proven and demonstrated. It should be noted that when comparing the results obtained with mycotoxins and data for specific substrates of each of the enzymes, close values of the angles of nucleophilic attack were obtained (see Tables 2-7). Comparing the obtained affinity values with each other and giving a rationale, we can say that there is catalysis in the active centers of enzymes with mycotoxin molecules. In fact, in the complex structure of the CbhA enzyme, the water molecule is in a convenient position for nucleophilic attack, since it is hydrogen bonded to the oxygen atoms of the Asp383 and Asp386 residues (see SI file, Figures S1-S4), located within 4.0 Å from the target C atom in the epoxide cycle of DON and T-2 toxin mycotoxin molecules. The function of the CbhA enzyme is to hydrolyze (1-4)-β-D-glucosidic bonds in cellulose and cellotetraose to release cellobiose. The Cbh9A enzyme is also an important cellulase with an inverting catalysis mechanism and high catalytic activity. Among the residues around subsites -1 and +1, Asp383, Asp386 and Glu795 are conserved across all family 9 enzymes as reported in study[44]. The carbohydrate moiety of glycosides is accompanied by an accompanying attack of the water molecule, which is activated by the base residue[45]. As is known, the lower the binding energy (kcal/mol), the higher the probability of ligand binding in the active center of the enzyme. To do this, it is necessary to compare the values of the obtained affinities in different EMVMSs, as the prevailing parameter, according to which it will be possible to assume the presence of enzymatic hydrolysis of the

https://doi.org/10.53964/jmbdd.2025005

Table 5. The Values of Nucleophilic Attack Angles and Distances Measured from the O Atom of the Corresponding Molecules to the C Atom in the Structures of Specific Substrates (S) - Hippurylphenyl Lactic Acid and 4-nitrophenyl Cellobioside, as well as from the O Atom of the Amino Acid Residues Glu270, Asp383, Asp386 to the H Atom of the Water Molecule in Active Centers of CPA, CbhA Enzymes in both EMVMSs

PyMol		UCSF Chimera		PyMol		UCSF Chimera	
Distances, Å	**Angle**	**Distances, Å**	**Angle**	**Distances, Å**	**Angle**	**Distances, Å**	**Angle**
Enzyme CPA (specific substrate S-hippurylphenyl-lactic acid)				Enzyme CbhA (specific substrate 4-nitrophenylcellobioside)			
H_2O---C= 1.7	H_2O--C--O= 111.1°	H_2O--C= 2.6	H_2O--C--O= 10[1]o	H_2O---C= 3.8	H_2O--C--O= 46.6[0]	H_2O---C=4.4	H_2O--C--O= 67°
Zn---H_2O=4.0		H_2O--Zn= 1.9		$O_{Asp383---H}$= 3.0		$O_{Asp383---H}$= 2.26	
O_{Glu270}--- H_{H2O}=4.0		O_{Glu270}---H_{H2O}= 1.8		$O_{Asp386---H}$= 2.7		$O_{Asp386---H}$= 1.9	

Table 6. Chemical Structures of Selected Ligands for Positive Control

Ligands	
4-chlorocinnamoyl-L-beta-phenyllactate (for CPA enzyme)	Cellatetraose (or (2R,3R,4R,5R)-4-[(2S,3R,4R,5S,6R)-5-[(2S,3R,4R,5S,6R)-3,4-dihydroxy-6-(hydroxymethyl)-5-[(2S,3R,4S,5S,6R)-3,4,5-trihydroxy-6-(hydroxymethyl)oxan-2-yl]oxyoxan-2-yl]oxy-3,4-dihydroxy-6-(hydroxymethyl)oxan-2-yl]oxy-2,3,5,6-tetrahydroxyhexanal for CbhA enzyme)

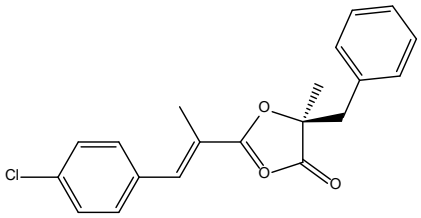

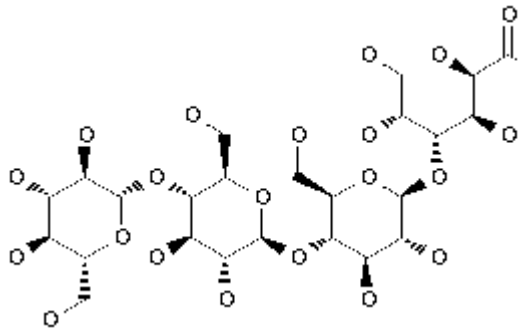

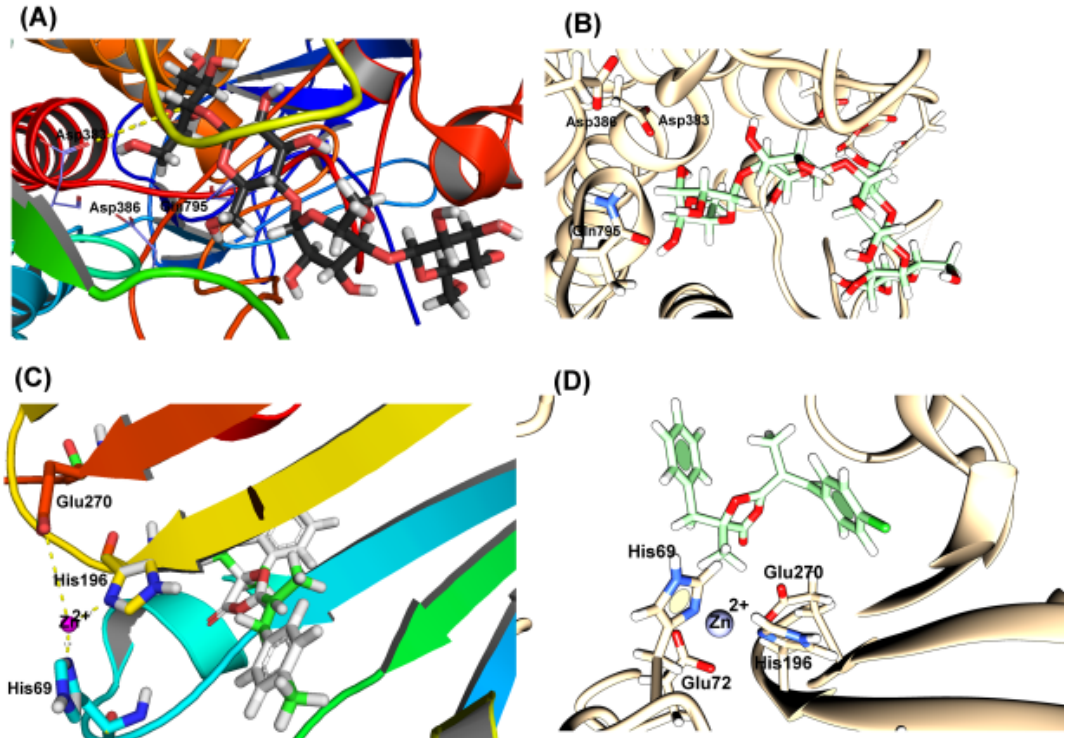

Figure 6. Binding of a Ligand Cellotetraose in the Active Site of the CPA Enzyme at the Optimum pH 7.5, Obtained using EMVMSs PyMol (A) and UCSF Chimera (B) and 4-chlorocinnamoyl-L-beta-phenyllactate in the Active Site of the CbhA Enzyme at the Optimal pH 6, Obtained using PyMol (C) and UCSF Chimera (D).

https://doi.org/10.53964/jmbdd.2025005

Table 7. The Values of Nucleophilic Attack Angles and Distances Measured from the O Atom of the Corresponding Molecules to the C Atom in the Structures of Specific Substrates 4-chlorocinnamoyl-L-beta-phenyllactate and Cellotetraose, as well as from the O Atom of the Amino Acid Residues Glu270, Asp383, Asp386 to the Zn Atom or to H Atom of the Water Molecule in Active Centers of CPA, CbhA Enzymes in both EMVMSs

PyMol		UCSF Chimera		PyMol		UCSF Chimera	
Distances, Å	Angle	Distances, Å	Angle	Distances, Å	Angle	Distances, Å	Angle
Enzyme CPA (ligand 4-chlorocinnamoyl-L-beta-phenyllactate)				Enzyme CbhA (ligand cellatetraose)			
C—Zn=4.4 H_2O—C=3.3	H_2O–C–O=35.2°	H_2O–C=2.6	H_2O–C–O=101°	H_2O—C=2.2	O_{Asp383}–C1–O_{CT1}=64.1°	H_2O—C=4.4	H_2O--C--O=67°
O_{Glu270}—Zn=4.1 Zn—H_2O=3.7		H_2O–Zn=1.9		$O_{Asp383—H}$=4.5	O_{Asp383}–C2–O_{CT1}=25.8°	$O_{Asp383—H}$=2.26	
O_{Glu270}—Zn=4.1		O_{Glu270}—H_{H2O}=1.8		$O_{Asp386—H}$=5.3		$O_{Asp386—H}$=1.9	

mycotoxin in one case or another.

Tables S1-S5 models can be identified that exactly correspond to those conformations of mycotoxins and specific substrates that are closest to the catalytic triad of the corresponding one. At the same time, it should be noted that the binding energy values of specific enzyme substrates are somewhat comparatively lower for the majority of ligand poses compared to the values obtained for mycotoxins.

Tables S6-S7 show the results of molecular docking of two selected ligands in the active centers of two enzymes. The results of the RMSD calculations confirm the docking protocol in addition to the results of the molecular docking of two specific enzyme substrates. Affinity describes the strength of molecular interactions. High affinity indicates strong binding between molecules, while low affinity suggests weaker binding.

When comparing the specific substrate of the enzyme CPA and the mycotoxin OTA, it is noticeable that for a large number of ligand poses, the obtained affinity values for ((S)-hippurylphenyl-lactic acid or (S)-2-(2-benzamidoacetyl) hydroxy-3-phenylpropanoic acid) are higher compared to the same values for the mycotoxin OTA - this is due to the poorer fit in the CPA active center for the mycotoxin compared to the specific substrate (see SI file - Tables S1 and S3).

In the case of the second enzyme CbhA and the mycotoxins DON and T-2 toxin, it can be said that the obtained negative values of the affinities of the specific substrate 4-nitrophenyl cellobioside for this compound are noticeably lower compared to the affinity values obtained for the mycotoxin DON and T-2 toxin, i.e. the specific substrate has a stronger interaction - higher affinity values with the active center of the enzyme than the mycotoxin DON due to the lack of catalytic complementarity of the mycotoxins compared to 4-nitrophenyl cellobioside (see SI file - Tables S2-S5).

But in comparison with the mycotoxin DON, the T-2 toxin was isolated with the obtained high affinities, i.e., low negative values compared to the same values for DON, which confirms the suggested strong interaction of the T-2 toxin in the active center of the enzyme compared to mycotoxins DON and OTA.

Reliable results are obtained when the stable mycotoxin and enzyme interact to produce higher affinities. In general, all affinities are different when molecular docking of mycotoxins is performed at the active sites of known enzymes (Table S8). It is known that the symmetry of the molecule must be taken into account in order to obtain an accurate RMSD value from molecular docking. For example, if the two benzene molecules completely overlaps each other, the RMSD value will be zero. If one molecule is then rotated along one of the symmetry axes until the two structures completely overlap again, their RMSD value should be zero due to the chemical identity of the structures[46].

Since the overlapping atoms are differently labeled between the two molecules in this example, naïve docking RMSD would have a nonzero value. Therefore, molecular symmetry needs to be taken into account in order to derive an accurate docking RMSD value. In many protein–ligand docking programs, a flexible small molecule structure is docked in a rigid protein receptor structure in order to find the optimal binding conformation and affinity of the small molecule within the protein binding pocket. Since the ability of these programs to accurately assess binding affinity is dependent on their ability to find the optimal conformation of the ligand in the protein binding pocket, docking programs are often benchmarked by their ability to reproduce the native binding pose of a ligand from a protein–ligand complex crystal structure. Computer-aided drug design, in particular protein–ligand docking, has brought about the discovery of many biologically active drugs[46].

A relative analysis of RMSD values highlights the flexibilities and dynamic behavior variations of enzymes during the simulation, recognizing the stability of the

complexes. This outcome supported the docking data, as the complexes displayed suitable docking scores and binding free energies.

It was pointed out in[47] that the presence of symmetrical functional groups (or symmetrical molecules) can lead to an increase in RMSD values. There is also information that small ligands give lower RMSD values than larger molecules. It is generally considered that assumptions of RMSD values within 2 Å are considered successful[48]. However, there is information that if the molecule contains symmetrical functional groups or is itself symmetrical, overestimated RMSD values may occur[49]. As indicated in[50], a number of features were considered for classifying proteins as rotationally symmetric or asymmetric, including RMSD, alignment length, and sequence identity. This ensures that rotationally symmetric structures always have higher RMSD values than asymmetric ones. As a rule, the accuracy of ligand docking in the active site of the enzyme is based on the RMSD values of all heavy atoms of the ligand in the docked position from those present in the crystal structure[51]. It was noted in[52] that the "positive positions" of ligand binding to the RMSD enzyme are less than 2 Å, and the "negative positions" of binding have an RMSD of more than 4 Å. These are the "positive or negative positions" of a ligand binding, depending on their presence at the active or presumably inactive site of the enzyme. The correct positions are designated as "positive", and those that go beyond the established limits - as "negative"[52].

In this regard, given the allowable RMSD range established above, for the mycotoxins used in this work, it would be more correct to take into account, in general, RMSD values that are in the range of 0-4 Å. The range of 0-4 Å in the case of the upper limit of RMSD (Table S4) corresponds to the first chosen model of DON binding in the case of using EMVMS UCSF Chimera, as well as the second and third models when binding T-2 toxin in the active site of the CbhA enzyme in the case of using both EMVMSs, than the fourth, ninth and second models for the OTA molecule, for which the values of the upper limit of RMSD are outside the above range. In the case of specific substrates, the upper limit of the RMSD for the molecule (S) - hippurylphenyl lactic acid, obtained using the PyMol molecular imaging system - does not meet this criterion. All standard deviation values that are obtained within 4 Å can be considered realistic, and exceeding this value is unlikely due to the impossibility, as expected, of the enzymatic hydrolysis of mycotoxins in the active sites of enzymes. As conformational flexibility is one of the most crucial factors affecting docking success, more work should be put into evaluating the conformational flexibility upon binding for a particular case in addition to developing new algorithms to replace the rigid body docking and scoring approach. Additionally, some of the molecular docking programs have been effective in predicting RMSDs ranging from 1.5 to 2 Å, depending on the experimental poses. However, flexible receptor docking, specifically receptor backbone flexibility, remains a challenge for contemporary docking programs.

The RMSD values for mycotoxins given in the final resulting Table S8 in accordance with affinities were chosen exclusively for the most advantageously located model or pose of mycotoxin, ligands and specific enzyme substrates in the active centers of enzymes. That is, these poses and models of mycotoxins were also chosen from the point of view of the distances and angles measured between certain atoms of the functional groups of mycotoxins and the atom of the closest catalytic residue of the enzyme.

5 CONCLUSION

Molecular docking plays a major role in academic and industrial drug screening and discovery processes. In recent years, significant improvement in high-performance computing, optimized software and environmental platforms, and enriched publicly accessible compound libraries have aided the computational screening methods to become more accurate, effective, and useful. It is a powerful tool for predicting the binding of ligands such as mycotoxins and specific enzyme substrates in the active binding site of an enzyme. Enzymatic degradation of mycotoxins, shown in AutoDock Vina with EMVMSs UCSF Chimera, PyMol, is one of the best approaches to study enzyme-mycotoxin interactions and to examine key protein-ligand interactions, including hydrogen bonds, hydrophobic interactions, and electrostatic contacts between ligands and amino acid residues in the target proteins. Due to the vast use of docking programs in the pharmaceutical industry, commercial packages that deal with docking are quite prevalent and are often used also by academic researchers.

In this scientific research, the AutoDock Vina program and UCSF Chimera and PyMol EMVMSs were used to suggest the possible enzymatic hydrolysis of mycotoxins OTA in the active site of the CPA enzyme, as well as T-2 toxin and DON in the active site of the CbhA enzyme at the optimal value The pH of the action of enzymes. Results with high affinities and RMSD values in the range of 0-4 Å can be considered reliable. Based on the results obtained as a result of molecular docking using EMVMSs UCSF Chimera and PyMol, it should be noted that T-2 toxin binds best in the active center of the CbhA enzyme - an affinity value of -7.8 kcal/mol. For the OTA mycotoxin, which binds better in the active site of the CPA enzyme, the affinity value is -7.1kcal/mol, and for the DON mycotoxin in the active site of the CbhA enzyme, the affinity value is -6.5kcal/mol at optimal pH values for the action of enzymes. Possible mechanisms of enzymatic hydrolysis based on docking poses of these mycotoxins were described.

Acknowledgements
Not applicable.

Conflicts of Interest
The authors declared no conflict of interest.

Data Availability
All data generated or analyzed during this study are included in this published article and its supplementary information files.

Author Contribution
Akhundov R. was responsible for the conceptualization, methodology of the study, and editing of the manuscript, for data analysis, writing and execution of the entire research work.

Abbreviation List
CbhA, Cellobiohydrolase
CPA, Carboxypeptidase A
DON, Deoxynivalenol
EMVMS, Extensible molecular visualization and modeling system
OTA, Ochratoxin A

References

[1] Zain ME. Impact of mycotoxins on humans and animals. Journal of Saudi chemical society, 2011; 15: 129-144.[DOI]
[2] Izco M, Vettorazzi A, Forcen R et al. Oral subchronic exposure to the mycotoxin ochratoxin A induces key pathological features of Parkinson's disease in mice six months after the end of the treatment. *Food Chem Toxicol*, 2021; 152: 112164.[DOI]
[3] Liu Y, Dong R, Yang Y et al. Protective effect of organic selenium on oxidative damage and inflammatory reaction of rabbit kidney induced by T-2 toxin. *Biol Trace Elem Res*, 2021; 199: 1833-1842.[DOI]
[4] Adhikari M, Negi B, Kaushik N et al. T-2 mycotoxin: toxicological effects and decontamination strategies. Oncotarget, 2017; 8: 33933-33952.[DOI]
[5] Azam MS, Yu D, Wu A. Enzymes for degradation of Fusarium mycotoxins. Food Safety & Mycotoxins. Springer Singapore: Singapore, 2019; 113-135.[DOI]
[6] Sandlin N, Russell Kish D, Kim J et al. Computational biology for enzymatic removal of mycotoxins. *OSFPreprint*, 2021; 2021: 1-22.[DOI]
[7] Forster MJ. Molecular modelling in structural biology. *Micron*, 2002; 33: 365-384.[DOI]
[8] Salmaso V, Moro S. Bridging molecular docking to molecular dynamics in exploring ligand-protein recognition process: An overview. *Front Pharmacol*, 2018; 9: 923.[DOI]
[9] Nahle S, El Khoury A, Savvaidis I et al. Detoxification approaches of mycotoxins: By microorganisms, biofilms and enzymes. *Int J Food Contam*, 2022; 9: 3.[DOI]
[10] Pettersen EF, Goddard TD, Huang CC et al. UCSF Chimera—a visualization system for exploratory research and analysis. *J Comput Chem*, 2004; 25: 1605-1612.[DOI]
[11] Goddard TD, Huang CC, Meng EC et al. UCSF ChimeraX: Meeting modern challenges in visualization and analysis. *Protein Sci*, 2018; 27: 14-25.[DOI]
[12] DeLano WL. Pymol: An open-source molecular graphics tool. *CCP4 Newsl Protein Crystallogr*, 2002; 40: 82-92.
[13] Rosignoli S, Paiardini A. Boosting the full potential of PyMOL with structural biology plugins. *Biomolecules*, 2022; 12: 1764.[DOI]
[14] Shelton V. Determining the Effectivity of PyMOL Approaches Through the Experimental Evaluation of Lactoferrin Binding, 2025.[DOI]
[15] Ford CT, Ullah S, Antunes DA et al. PyMOLfold: Interactive Protein and Ligand Structure Prediction in PyMOL. arXiv preprint arXiv:2502.00508, 2025.[DOI]
[16] Brunger AT, Wells JA. DeLano 21 June 1972–3 November 2009. *Nat Struct Mol Biol*, 2009; 16: 1202-1203.[DOI]
[17] Goddard TD, Huang CC, Ferrin TE. Visualizing density maps with UCSF Chimera. *J Struct Biol*, 2007; 157: 281-287.[DOI]
[18] Meng EC, Pettersen EF, Couch GS et al. Tools for integrated sequence-structure analysis with UCSF Chimera. *BMC bioinformatics*, 2006; 7: 339.[DOI]
[19] Pettersen EF, Goddard TD, Huang CC et al. UCSF ChimeraX: Structure visualization for researchers, educators, and developers. *Protein Sci*, 2021; 30: 70-82.[DOI]
[20] Ramírez-Villarreal J, Álvarez-Martínez R. Application of I TASSER, trRosetta, UCSF Chimera, HADDOCK server, and HEX loria for De Novo and In Silico Design of Proteins. *J Vis Exp*, 2025; 221: e680033.[DOI]
[21] Agu PC, Afiukwa CA, Orji OU et al. Molecular docking as a tool for the discovery of molecular targets of nutraceuticals in diseases management. *Sci Rep*, 2023; 13: 13398.[DOI]
[22] Kerwin SM. ChemBioOffice Ultra 2010 Suite. *J Am Chem Soc*, 2010; 132: 2466-2467.[DOI]
[23] Kolossvary I, Guida WC. Comprehensive conformational analysis of the four-to twelve-membered ring cycloalkanes: identification of the complete set of interconversion pathways on the MM2 potential energy hypersurface. *J Am Chem Soc*, 1993; 115: 2107-2119.[DOI]
[24] Stewart JJP. Optimization of Parameters for Semi-Empirical Methods. *J Comput Chem,* 1989; 10: 503-513.[DOI]
[25] Morris GM, Huey R, Lindstrom W et al. AutoDock4 and AutoDockTools4: Automated docking with selective receptor flexibility. *J Comput Chem*, 2009; 30: 2785-2791.[DOI]
[26] Trott O, Olson AJ. AutoDock Vina: improving the speed and accuracy of docking with a new scoring function, efficient optimization, and multithreading. *J Comput Chem*, 2010; 31: 455-461.[DOI]
[27] Tang S, Chen R, Lin M et al. Accelerating autodock vina with gpus. *Molecules*, 2022; 27: 3041.[DOI]
[28] Bugnon M, Röhrig UF, Goullieux M et al. SwissDock 2024: major enhancements for small-molecule docking with Attracting Cavities and AutoDock Vina. *Nucleic Acids Res*, 2024; 52: W324-W332.[DOI]
[29] Buccheri R, Rescifina A. High-Throughput, High-Quality: Benchmarking GNINA and AutoDock Vina for Precision Virtual Screening Workflow. *Molecules*, 2025; 30: 3361.[DOI]
[30] Baker NA, Sept D, Joseph S et al. Electrostatics of

nanosystems: application to microtubules and the ribosome. *Proc Natl Acad Sci*, 2001; 98: 10037-10041.[DOI]

[31] Dolinsky TJ, Czodrowski P, Li H et al. PDB2PQR: expanding and upgrading automated preparation of biomolecular structures for molecular simulations. *Nucleic Acids Res*, 2007; 35: W522-W525.[DOI]

[32] Elgammala WE, Elkady H, Mahdy HA et al. Rationale Design and Synthesis of Novel Apoptotic Thiadiazole Analogues Targeting VEGFR-2: Computational and In *vitro* studies. *RSC Advances*, 2023; 13; 51: 35853-35876.[DOI]

[33] Kupski L, Queiroz MI, Badiale-Furlong E. Application of carboxypeptidase A to a baking process to mitigate contamination of wheat flour by ochratoxin A. *Process Biochem*, 2018; 64: 248-254.[DOI]

[34] Pitout MJ. A rapid spectrophotometric method for the assay of carboxypeptidase A. *Biochem Pharmacol*, 1969; 18: 1829-1835.[DOI]

[35] Wu S, Zhang C, Xu D et al. Catalysis of carboxypeptidase A: promoted-water versus nucleophilic pathways. *J Phys Chem B*, 2010; 114: 9259-9267.[DOI]

[36] Lee M, Kim DH. Hippuryl-α-methylphenylalanine and hippuryl-α-methylphenyllactic acid as substrates for carboxypeptidase A. Syntheses, kinetic evaluation and mechanistic implication. Bioorganic & medicinal chemistry, 2000; 8: 815-823.[DOI]

[37] Schubot FD, Kataeva IA, Chang J et al. Structural basis for the exocellulase activity of the cellobiohydrolase CbhA from *Clostridium thermocellum*. *Biochemistry*, 2004; 43: 1163-1170.[DOI]

[38] Kataeva I, Li XL, Chen H et al. Cloning and sequence analysis of a new cellulase gene encoding CelK, a major cellulosome component of *Clostridium thermocellum*: evidence for gene duplication and recombination. *J Bacteriol*, 1999; 181: 5288-5295.[DOI]

[39] Banci L, Bertini I, La Penna G. A molecular dynamics study of carboxypeptidase A: effect of protonation of Glu 270. *Inorg Chem*, 1993; 32: 2207-2211.[DOI]

[40] Castro-Alvarez A, Costa AM, Vilarrasa J. The performance of several docking programs at reproducing protein–macrolide-like crystal structures. *Molecules*, 2017; 22: 136.[DOI]

[41] Boittier ED, Tang YY, Buckley MKE et al. Assessing molecular docking tools to guide targeted drug discovery of CD38 inhibitors. *Int J Mol Sci*, 2020; 21: 5183.[DOI]

[42] Koeck DE, Wibberg D, Maus I et al. Complete genome sequence of the cellulolytic thermophile *Ruminoclostridium* cellulosi wild-type strain DG5 isolated from a thermophilic biogas plant. *J Biotechnol*, 2014; 188: 136-137.[DOI]

[43] Song JB, Hah SS, Suh JH. Cyclen-containing inhibitors of carboxypeptidase A synthesized in search of target-selective artificial proteases. *Bull Korean Chem Soc*, 2004; 25: 1703-1706.[DOI]

[44] Han F, Liu Y, E J et al. Effects of Tyr555 and Trp678 on the processivity of cellobiohydrolase A from *Ruminiclostridium thermocellum*: A simulation study. *Biopolymers*, 2018; 109: e23238.[DOI]

[45] Davies G, Henrissat B. Structures and mechanisms of glycosyl hydrolases. *Structure*, 1995; 3: 853-859.[DOI]

[46] Bell EW, Zhang Y. Dock RMSD: an open-source tool for atom mapping and RMSD calculation of symmetric molecules through graph isomorphism. *J Cheminfor*, 2019; 11: 40.[DOI]

[47] Ding Y, Fang Y, Moreno J et al. Assessing the similarity of ligand binding conformations with the Contact Mode Score. *Comput Biol Chem*, 2016; 64: 403-413.[DOI]

[48] Park H, Zhou G, Baek M et al. Force field optimization guided by small molecule crystal lattice data enables consistent sub-angstrom protein–ligand docking. *J Chem Theory Comput*, 2021; 17: 2000-2010.[DOI]

[49] Allen WJ, Rizzo RC. Implementation of the Hungarian algorithm to account for ligand symmetry and similarity in structure-based design. *J Chem Inf Model*, 2014; 54: 518-529.[DOI]

[50] Myers-Turnbull D, Bliven SE, Rose PW et al. Systematic detection of internal symmetry in proteins using CE-Symm. *J Mol Biol*, 2014; 426: 2255-2268.[DOI]

[51] Xiao W, Wang D, Shen Z et al. Multi-body interactions in molecular docking program devised with key water molecules in protein binding sites. *Molecules*, 2018; 23: 2321.[DOI]

[52] Morrone JA, Weber JK, Huynh T et al. Combining docking pose rank and structure with deep learning improves protein–ligand binding mode prediction over a baseline docking approach. J Chem Inf Model, 2020; 60: 4170-4179.[DOI]